Eigenstate Fokker-Planck equation for magnetic nanostructures

Zhuonan Lin [1,2,3] and Vitaliy Lomakin [1,2,*]

[1] *Department of Electrical and Computer Engineering, University of California San Diego, La Jolla, California 92093, USA*
[2] *Center for Memory and Recording Research, La Jolla, California 92093, USA*
[3] *Materials Science and Engineering Program, University of California San Diego, La Jolla, California 92093, USA*

(Received 21 December 2024; accepted 16 June 2025; published 14 August 2025)

A Fokker-Planck equation (FPE) approach is presented to calculate the magnetization probability densities in nanomagnetic systems characterized by complex magnetization dynamics. The formulation is based on an eigenstate expansion of the solutions of the linearized Landau-Lifshitz-Gilbert equation (LLGE), which allows considering statistical properties of nonuniform magnetization dynamics, such as finding write error rates in spin transfer torque magnetic random access memories induced by thermal noise. The formulation includes finding eigenstates and eigenfrequencies of the structure of interest, formulating an FPE describing the probability density dynamics of the excitation coefficients of the eigenstate solutions, and using this equation to find derived quantities. Compared to using the stochastic LLGE, the presented approach directly obtains statistical properties. Compared to generally used FPE approaches, the presented formulation allows handling nonuniform dynamics. The formulation of using the eigenstate-based FPE is applicable to many types of physics.

DOI: 10.1103/prk5-s1y1

I. INTRODUCTION

Stochastic dynamics caused by thermal effects is an inherent characteristic of physical systems. For example, stochastic effects lead to Brownian motion [1], radioactive decay [2], and fluid turbulence [3]. Stochastic effects in magnetic nanostructures cause magnetization fluctuations, leading to a number of phenomena, such as ferromagnetic resonance broadening [4] and spontaneous magnetization switching [5]. Stochastic dynamics affects the operation of various magnetic structures and devices. Thermal effects play an important role in the switching properties of magnetic tunnel junctions (MTJs) used in spin transfer torque (STT) magnetoresistive random access memories [6]. Thermal fluctuations result in probabilistic switching, leading to write errors, characterized by a write error rate (WER) [6,7] for a given switching current pulse duration or by a distribution of the switching time for a given current strength.

Statistical properties of the stochastic dynamics caused by thermal fluctuations in general physical systems can be obtained by solving dynamic equations for a large ensemble of realizations. However, such an approach can be computationally expensive or impossible and provides limited physical insights. Various methods can account for stochastic behavior, such as rare event enhancement [8] and machine learning assistance [9]. However, these approaches still pose challenges to obtain statistical properties. An alternative approach is to formulate a Fokker-Planck equation (FPE), which provides a solution directly for the probability density function (PDF) [10,11]. FPE was formulated for magnetic elements, including MTJs, based on a macrospin model for which the PDF is only a function of two angles [7,12]. Such an approximation is only valid for magnetic elements that are small compared to the exchange length. Most structures are greater than the exchange length and their magnetization dynamics is spatially nonuniform. Using macrospin-based FPE for such cases is inaccurate. Extending FPE formulations to structures with spatially nonuniform dynamics is essential for comprehending and leveraging their statistical properties.

Here, we introduce an FPE constructed based on an eigenstate expansion of the magnetization obtained via a linearized Landau-Lifshitz-Gilbert equation (LLGE). It allows statistical dynamic properties of the magnetization to be obtained, including complex spatial variations and STT effects. We demonstrate an example application to obtain WER of thermally affected magnetization switching in MTJs. The introduced approach is general, and the formulated FPE applies to various areas of physics, e.g., statistical properties of lasers [10,13], temperature-dependent magnetic or electric susceptibility under time-dependent external fields [14,15], or dynamics in mechanical systems [16,17].

Consider magnetization dynamics in a magnetic structure that may be driven by the STT or spin Hall effect and is subject to stochastic temperature effects. The dynamics is described in general by the stochastic LLGE [18], which is nonlinear in $\mathbf{m}$. The LLGE can be linearized by representing the magnetization $\mathbf{m} = \mathbf{m}_0 + \mathbf{v}$, where $\mathbf{m}_0$ is the equilibrium magnetization state and $\mathbf{v}$ is a small magnetization deviation around $\mathbf{m}_0$ [19]. This is allowed when the magnetization varies insignificantly around its equilibrium state. Weak magnetization variations

*Contact author: vlomakin@ucsd.edu

can be due to weak excitations, e.g., by weak applied fields or by STT. The variations are also weak in the initial stages of the magnetization dynamics near an equilibrium state even when the system is driven by strong excitations, e.g., an onset of switching by STT, which proceeds eventually with a nonlinear switching. The corresponding dynamics, including stochastic thermal excitations, provides statistical properties, which accurately describe weak-signal behavior and may serve as a good approximation even when nonlinear dynamics occurs.

II. EIGENSTATE FOKKER-PLANCK EQUATION

A. Linearized Landau-Lifshitz-Gilbert equation

Linearized LLGE [19] can be written in the following form:

$$\frac{\partial \mathbf{v}}{\partial t} = A\mathbf{v} + \mathbf{F}_d + \mathbf{F}_s. \tag{1}$$

Here, A is a linear operator, $\mathbf{F}_d$ is a deterministic force term related to STT excitation, and $\mathbf{F}_s$ is the stochastic term related to thermal stochastic effects. This form applies to various physical systems, e.g., Maxwell's equations, state equations for laser systems, mechanical equations of motion, and equations of elasticity. In different physics types, the small perturbation would have a different physical meaning, e.g., electromagnetic fields, pressure, mechanical displacement, or strain. The linear operator A may include differential and integral components that describe different physical interactions and complex spatial variations in the system [19]. For various physical systems, the force term can be related to different source terms, such as charge current, spin current, or mechanical force. The stochastic term is related to thermal excitations that are typically characterized by white noise [18].

For the LLGE, the linear operator can be given by

$$\begin{aligned} A &= \Lambda(\mathbf{m}_0)[A_0 + \alpha\Lambda(\mathbf{m}_0)A_0 - \gamma\beta\Lambda(\mathbf{p})],\\ A_0 &= [(\mathbf{H}_0\cdot\mathbf{m}_0)I - C]. \end{aligned} \tag{2}$$

Here, I is the unit operator, $\Lambda(\mathbf{u})\mathbf{v} = \mathbf{u}\times\mathbf{v}$ is a rotation operator, γ is the gyromagnetic ratio, and α is the damping constant. The field $\mathbf{H}_0 = \mathbf{H}_{\text{eff}}(\mathbf{m}_0)$ is the equilibrium effective magnetic field, satisfying Brown's condition [20]. The linear operator C determines the effective dynamic magnetic field as $\mathbf{H}_{\text{eff}}(\mathbf{v}) = C\mathbf{v}$. Effective magnetic fields include the magnetostatic, exchange, and anisotropy field components. Due to the Λ operator, $\mathbf{v}$ is normal to $\mathbf{m}_0$, so $\mathbf{v}$ has only two independent components at every spatial location, and the operators are understood within this property [21]. Furthermore, the terms β and $\mathbf{p}$ determine the STT field $\mathbf{H}_{\text{stt}} = \beta\Lambda(\mathbf{p})$, where $\mathbf{p}$ is the direction of polarization and $\beta = Ib$ is an STT parameter with the electric current I and the coefficient b related to spintronic excitations [22–24]. STT allows overcoming the magnetic damping and, e.g., for structures with two equilibrium states, can lead to switching when the current I is large enough. The current density that leads to switching at zero temperature in infinite time is referred to as the critical current I_c.

The deterministic and stochastic driving terms are given by

$$\begin{aligned} \mathbf{F}_d &= -\gamma\beta\Lambda(\mathbf{m}_0)\Lambda(\mathbf{m}_0)\mathbf{p},\\ \mathbf{F}_s &= [\gamma\Lambda(\mathbf{m}_0) + \alpha\gamma\Lambda(\mathbf{m}_0)\Lambda(\mathbf{m}_0)]\mathbf{H}_{\text{th}}. \end{aligned} \tag{3}$$

The field $\mathbf{H}_{\text{th}}$ represents thermal fluctuations as white noise described by a normal distribution with zero mean and the dispersion $\sigma_{\mathbf{H}} = \sqrt{(2\alpha k_B T)/(\gamma V M_s)}$, where T is the temperature, k_B is the Boltzmann constant, V is the effective volume, e.g., the volume of a discretization element or a small particle, and M_s is the saturation magnetization [18].

B. Eigenstate representation

Equation (1) can be solved for general structures either directly or via the eigenstate expansion [19]

$$\mathbf{v} = \sum_n \mathbf{v}_n = 2\,\mathrm{Re}\left[\sum_n a_n(t)\varphi_n(\mathbf{r})\right], \tag{4}$$

where $\{\omega_n, \varphi_n\}$ are the eigenfrequencies and eigenstates of the eigenvalue problem $A\varphi_n = j\omega_n\varphi_n$, $\mathbf{v}_n$ is nth solution component corresponding to the nth eigenstate, and a_n is the complex-valued time-dependent amplitude. The eigenfrequencies are complex, i.e., $\omega_n = \omega_n' + j\omega_n''$. The time-dependent amplitudes are solutions to the time-domain differential equations [19]

$$\frac{da_n}{dt} = j\omega_n a_n + P_n^d + P_n^s, \tag{5}$$

where

$$P_n^d = \langle \mathbf{F}_d, A_0\varphi_n\rangle \quad \text{and} \quad P_n^s = \langle \mathbf{F}_s, A_0\varphi_n\rangle \tag{6}$$

are forcing terms corresponding to the deterministic and stochastic components in the LLGE (1) with the inner product $\langle\cdot,\cdot\rangle$ defined as the volume integral over the structure domain. The stochastic noise term P_n^s is complex valued. It is a linear transform of $\mathbf{H}_{\text{th}}$, so it also follows a normal distribution. The standard deviations of the real and imaginary parts of P_n^s are given by

$$\begin{aligned} \sigma_n^r(P_n^s) &= \mathrm{Re}\left(\sigma_{\mathbf{H}}\langle A_s^T A_0\varphi_n, \mathbf{1}\rangle\right),\\ \sigma_n^i(P_n^s) &= \mathrm{Im}\left(\sigma_{\mathbf{H}}\langle A_s^T A_0\varphi_n, \mathbf{1}\rangle\right), \end{aligned} \tag{7}$$

where A_s^T is the transpose of A_s and $\mathbf{1}$ is a unit vector. The nonuniform dynamics is automatically accounted for by the fact that the eigenstates are spatially nonuniform. Statistical properties can be obtained by solving Eq. (5) repetitively to obtain a sufficient ensemble of realizations. Such a brute-force approach may require finding many realizations that often is impossible to accomplish, e.g., small and large values of WERs in MTJs. Additionally, the brute-force approach provides limited insight into the physics of stochastic dynamics. To address these difficulties, we formulate an FPE as a counterpart of Eq. (5), which can be regarded as a Langevin equation [10], for PDF corresponding to the coefficients $a_n(t)$.

C. Fokker-Planck equation

Equation (5) can be viewed as a Langevin equation [10]. We can write the complex-valued amplitude a_n in polar form as $a_n = |a_n|e_n^{j\phi}$, where $|a_n|$ is the complex magnitude and ϕ_n is the complex phase. We use the Kramers-Moyal expansion [11] to rewrite Eq. (5) as a multidimensional Langevin equation [10] for $|a_n|$ and ϕ_n:

$$\frac{d|a_n|}{dt} = h_1 + \sum_{i=i}^{2} g_{1i} P_n^s(t)_i, \quad \frac{d\phi_n}{dt} = h_2 + \sum_{i=1}^{2} g_{2i} P_n^s(t)_i, \tag{8}$$

where the sum index $i = 1, 2$ is over the real and imaginary parts of the complex variables, and the random variables are $P_n^s(t)_1 = \mathrm{Re}(P_n^s)$ and $P_n^s(t)_2 = \mathrm{Im}(P_n^s)$. The coefficients g_{1i}, g_{2i}, h_1, and h_2 are obtained from Eq. (5) as

$$\begin{aligned} h_1 &= -\omega_n^i |a_n| + \mathrm{Re}\left(P_n^d\right)\cos\phi_n + \mathrm{Im}\left(P_n^d\right)\sin\phi_n, \\ h_2 &= \omega_n^r + \frac{1}{|a_n|}\left[\mathrm{Im}\left(P_n^d\right)\cos\phi_n - \mathrm{Re}\left(P_n^d\right)\sin\phi_n\right], \\ g_{11} &= \cos\phi_n, \quad g_{12} = \sin\phi_n, \\ g_{21} &= -\sin\phi_n/|a_n|, \quad g_{22} = \cos\phi_n/|a_n|, \end{aligned} \tag{9}$$

where $\omega_n^r = \mathrm{Re}(\omega_n)$ and $\omega_n^i = \mathrm{Im}(\omega_n)$ are the real and imaginary parts of the complex normal frequency of the nth mode.

We define a time-dependent PDF $\rho_n(|a_n|, \phi_n; t)$ for the magnitude and phase coefficients $|a_n|$ and ϕ_n. The FPE can then be obtained based on the Kramers-Moyal expansion [10]:

$$\frac{\partial}{\partial t}\rho_n = -\sum_{p=1}^{2} \frac{\partial}{\partial \xi_p}\left(D_p^{(1)}\rho_n\right) + \sum_{p,q=1}^{2} \frac{\partial}{\partial \xi_p \partial \xi_q}\left(D_{pq}^{(2)}\rho_n\right), \tag{10}$$

where $\xi_1 = |a_n|$ and $\xi_2 = \phi_n$ are the two random variables. The coefficients $D_p^{(1)}(|a_n|, \phi_n)$ and $D_{pq}^{(2)}(|a_n|, \phi_n)$ are obtained from the Kramers-Moyal expansion:

$$D_p^{(1)} = h_p + \sum_{i,q=1}^{2} g_{qi} \frac{\partial}{\partial \xi_q} g_{pi}, \quad D_{pq}^{(2)} = \sum_{i=1}^{2} g_{pi} g_{qi}, \tag{11}$$

where the coefficients g_{1i}, g_{2i}, h_1 and h_2 are defined in Eq. (9), and the sum index $i = 1, 2$ is over the real and imaginary parts of the complex variables. Solving the FPE gives the time-dependent PDF of time coefficients of each eigenstate. The PDF of the spatial solution can be obtained based on the PDFs of eigenstate coefficients.

The FPE can be solved using the periodicity condition $\phi_n(0) = \phi_n(2\pi)$ for phase ϕ_n and the zero flux boundary condition $(\partial|a_n|/\partial \mathbf{n}) = 0$ for $|a_n|$.

The solution requires an initial condition, i.e., $\rho_n(|a_n|, \phi_n; t = 0)$. To that end, we first consider the system without the driving term P_n^d and find the analytical solution to Eq. (5) with $P_n^d = 0$:

$$a_n(t) = e^{j\omega_n t}\left[\int_0^t e^{-j\omega_n \tau} P_n^s(\tau) d\tau + a_n(0)\right]. \tag{12}$$

The initial condition should be the system starting from equilibrium state in the finite temperature for infinite time, so that $a_n(0) = 0$ and $t \to \infty$ in Eq. (12), which leads to

$$\left[\sigma_n^r(a_n)\right]^2 = \frac{1}{4\omega_n^i\left({\omega_n^i}^2 + {\omega_n^r}^2\right)}\left\{\left(2{\omega_n^i}^2 + {\omega_n^r}^2\right)\left[\sigma_n^r\left(P_n^s\right)\right]^2 + {\omega_n^r}^2\left[\sigma_n^i\left(P_n^s\right)\right]^2\right\},$$

$$\left[\sigma_n^i(a_n)\right]^2 = \frac{1}{4\left(\omega_n^i\right)\left({\omega_n^i}^2 + {\omega_n^r}^2\right)}\left\{\left(2{\omega_n^i}^2 + {\omega_n^r}^2\right)\left[\sigma_n^i\left(P_n^s\right)\right]^2 + {\omega_n^r}^2\left[\sigma_n^r\left(P_n^s\right)\right]^2\right\}. \tag{13}$$

Since both the real and imaginary parts of a complex random variable ($\mathrm{Re}\{P_n^s\}$ and $\mathrm{Im}\{P_s^n\}$) follow the normal distribution, its magnitude follows the Rayleigh distribution, and the phase follows the uniform distribution [11]. As a result, the joint distribution, viz., the initial condition, is given by

$$\rho_n(|a_n|, \phi_n; 0) = \frac{|a_n| \exp\left[-\frac{1}{2}|a_n|^2\left(\frac{\cos^2\phi_n}{\sigma_n^{r2}} + \frac{\sin^2}{\phi_n}{\sigma_n^i}^2\right)\right]}{2\pi\sigma_n^r\sigma_n^i}, \tag{14}$$

where σ_n^r and σ_n^i are the normal distribution standard deviations of $\mathrm{Re}(a_n)$ and $\mathrm{Im}(a_n)$, respectively.

The eigenvalue-based FPE formulation allows for the obtaining of various statistical properties based on the PDF and can be used in various areas of physics. The approach provides statistical solutions directly without the need to solve Eq. (1) for a massive number of realizations. It reduces the number of degrees of freedom from a fully discretized space to the space of direct PDF solutions for the eigenstate coefficients. For a set of uses, one may require only a small number of eigenstate solutions to be taken into account. In linear response considerations, only the eigenstate with the frequency of excitation near a particular eigenfrequency plays a role. An example of such a linear response system is the temperature-dependent magnetic or electric susceptibility of freestanding or arrayed magnetic, dielectric, or plasmonic nanoparticles that support complex spatially nonuniform eigenstates [19]. Other examples may include noise in nanoscale devices [25] or linear magnetic spin waves [26]. In other cases, including nonlinear ones, often only certain linearized eigenstates may play a dominant role, e.g., in the MTJ switching process [19]. The number of eigenstates that need to be accounted for may increase with the considered system size, but the presented approach still provides a way to solve complex practical problems that otherwise are impossible.

D. Use for write error rates in MTJs

We now present results of using the FPE framework for obtaining thermal statistical switching properties of MTJs driven by STT. The MTJ is composed of a disk-shaped free layer of 1 nm thickness and diameters (D) of 20 and 80 nm [Fig. 1(a)]. The material parameters are for the effective perpendicular uniaxial anisotropy energy density $K_U = 6.11$ Merg/cm^3, saturation magnetization $M_s = 960$ emu/cm^3, exchange stiffness $A_{\mathrm{ex}} = 1$ μerg/cm, and damping constant $\alpha = 0.01$. STT is present at the bottom surface of the disk related to the corresponding reference layer. The MTJ example is chosen as a complex case that includes nonuniform magnetization and demonstrates that the linearized approach provides a good approximation to nonlinear switching properties. For these MTJs, the magnetization dynamics becomes highly nonuniform at sizes greater than the domain wall width, which corresponds to diameters greater than 20 nm. In addition, for such sizes, the energy barrier becomes large. Using single-spin-based FPE

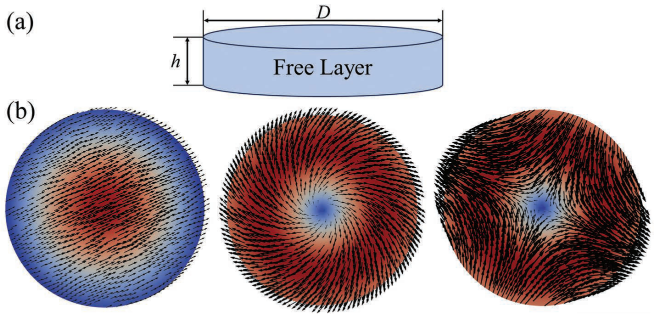

FIG. 1. (a) Illustration of an MTJ free layer disk, where h is the height and D is the diameter of the disk. (b) First three eigenstates for $D = 80$ nm. The color and arrows represent the magnitude and real part, respectively.

approaches of direct stochastic simulations [7,12], for such cases, is not valid and using brute-force stochastic simulations is impractical or impossible.

The first several eigenstates for this structure are shown in Fig. 1(b). The corresponding eigenfrequencies and critical current densities at zero temperature are shown in Table I. The first eigenstate is most spatially uniform, but still is nonuniform, and it has the smallest eigenfrequency and critical current density. The other eigenstates are highly nonuniform and have higher critical currents. The significance of the critical current per eigenstate, I_c^n, is that for $I > I_c^n$, $\omega_n'' < 0$, and the corresponding amplitude increases exponentially over time; i.e., it becomes active. This leads to an increase of the magnetization deviation and eventually switching occurs via a nonlinear process, often by domain wall. These active eigenstates are most important for the switching process, and typically, there is only a small number of them; in the presented case, there are only one to three active eigenstates.

An important example of a derived statistical quantity is WER. For WERs in perpendicular MTJs, we characterize the switching behavior by the magnitude of the spatially averaged in-plane magnetization [19,27], which at the initial dynamics stage is approximately given by the magnitude of the spatially averaged magnetization deviation $|\bar{\mathbf{v}}|$. A nonswitching condition can be defined as $|\bar{\mathbf{v}}| \leqslant s$, where $s = O(1)$ is a certain critical value. Using Eq. (10), the time-dependent WER for the system is given by the integral of the joint probabilistic density function of n active eigenstates:

$$\mathrm{WER}(t) = \int \cdots \int_{|\bar{\mathbf{v}}| \leqslant s} \rho(a_1 \cdots a_n; t) da_1 \cdots da_n. \quad (15)$$

TABLE I. Eigenfrequency (f') and critical current (I_c) of first four eigenstates (denoted by n) for $D = 20$ and 80 nm, respectively.

	n	1	2	3	4
$D = 20$ nm	f_n' (GHz)	8.13	29.71	29.81	65.55
	I_c^n (μA)	2.67	9.74	9.77	21.42
$D = 80$ nm	f_n' (GHz)	3.76	5.80	5.86	8.63
	I_c^n (μA)	19.60	30.15	30.66	45.24

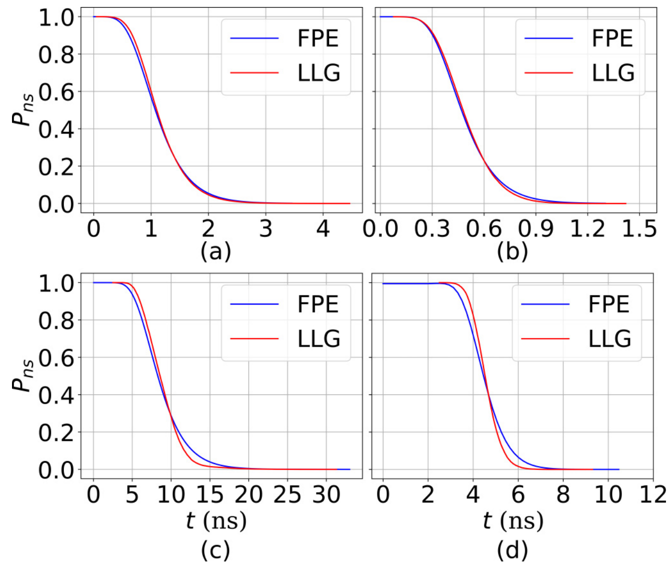

FIG. 2. WER via the stochastic LLGE and FPE for $T = 300$ K for (a) $D = 20$ nm, $I = 9.5$ μA, (b) $D = 20$ nm, $I = 21$ μA, (c) $D = 80$ nm, $I = 29.5$ μA, and (d) $D = 80$ nm, $I = 45$ μA.

To determine the upper limit of integration, we consider the approximation in which the total magnetization deviation consists of each eigenstate component $\bar{\mathbf{v}} = \sum_n \bar{\mathbf{v}}_n$. We consider condition $\bar{\mathbf{v}}_n \leqslant s_n$, where s_n is the critical value for the nth component and $s = \sum_n s_n$ for each eigenstate. Then, the nonswitching probability of nth eigenstate P_n is given by

$$P_n(t) = \int_0^{s_n} \int_0^{2\pi} \rho(|a_n|, \phi_n; t) d|a_n| d\phi_n. \quad (16)$$

The WER is the total nonswitching probability combined of all the eigenstate contributions:

$$\mathrm{WER}(t) = \sum_{s_n} \prod_n P_n(t). \quad (17)$$

As a demonstration of using the presented framework, we consider WERs due to the magnetization switching at room temperature in an MTJ with perpendicular magnetic anisotropy. The geometry and material parameters of the MTJ are the same as in Fig. 1 and Table I. We found eigenstates by discretizing the system via the finite element method [28] with Arnoldi's method [29]. The results of the eigensolver indicate the active modes involved in the switching process, where the imaginary parts of the eigenfrequencies are negative [19]. We use the presented FPE formulation to calculate the PDF and WER. The FPE is solved numerically [30,31]. To validate the formulation, we compare the FPE-based results to the results obtained via a massive set of micromagnetic simulations directly solving the stochastic LLGE. We note that such a comparison is only possible for intermediate values of the WER, still requiring many simulation hours on a large computer cluster. However, for small and large values of the WER, such simulations are practically impossible because of the prohibitively large number of calculated realizations required. FPE can be used for any value of the WER using any computing system.

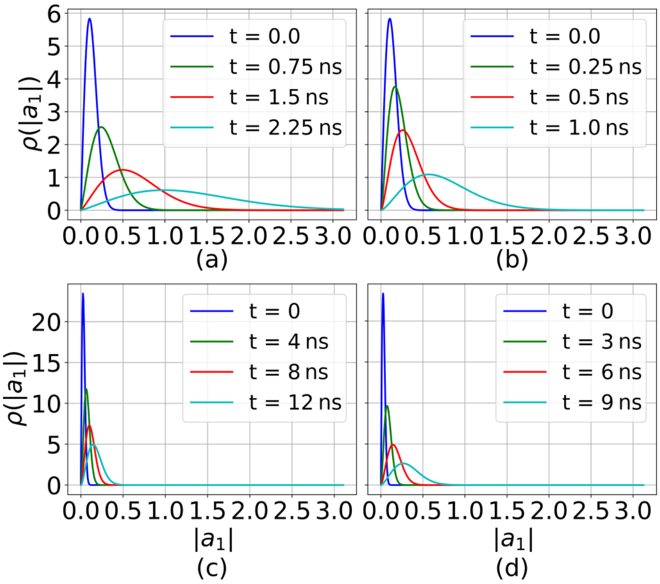

FIG. 3. PDF for $|a_1|$ for $T = 300$ K for (a) $D = 20$ nm, $I = 9.5$ μA, (b) $D = 20$ nm, $I = 21$ μA, (c) $D = 80$ nm, $I = 29.5$ μA, and (d) $D = 80$ nm, $I = 45$ μA.

WER and marginal PDF in Figs. 2 and 3 are shown for MTJ of two sizes, $D = 20$ nm and $D = 80$ nm. For the smaller size ($D = 20$ nm), the magnetization switching is more uniform and the switching is mostly by a uniform magnetization rotation. For the greater MTJ size, the magnetization is more nonuniform and the magnetization switching is by domain wall. However, in both cases, the initial magnetization dynamics is due to the excitation of active eigenstates [19]. The results are shown for the currents that correspond to a single active mode for $D = 20$ nm and one or three active modes for $D = 80$ nm, as follows from Table I. The higher active modes are highly nonuniform and their contribution is found to be more significant for the large-sized MTG, which is attributed to the fact that their critical currents are closer to each other.

Figure 2 also shows the WER obtained by the FPE approach and by running a massive set of micromagnetic simulations with stochastic thermal field. We find a good agreement in both cases with a slightly better agreement for the smaller MTJ case. We note that for the larger current cases, there are more active modes that need to be accounted for; otherwise, the results would differ. Figure 3 shows the marginal PDF for $|a_1|$, which is used to obtain the WER results in Fig. 2. The PDF width increases with time, which corresponds to a higher probability of switching and a higher WER in Fig. 2.

III. SUMMARY

In summary, this work presented an FPE approach to calculate PDF and its derivative quantities, such as WER, in systems with complex spatially nonuniform dynamics. The approach is based on an eigenstate expansion of the magnetization spatial distribution using the linearized LLGE. The eigenstate representation allows for accounting for spatially nonuniform dynamics with only a small number of degrees of freedom, thus overcoming the need of multidimensional solution space that otherwise would be required if using FPE with direct spatial discretization, in which each spatial site is taken as a degree of freedom. The examples presented demonstrate the power of the approach for the computing of WER in MTJs in terms of providing physical insights into the stochastic magnetization dynamics and major enhancement of the computational capabilities. This FPE framework of this framework is general and can be extended to other physical systems in which stochastic dynamics with spatial nonuniformity is of interest. Additionally, the framework can be extended to nonlinear interactions based on eigenstate expansions [32], e.g., to obtain thermally induced probability of power transfer between different modes.

ACKNOWLEDGMENTS

This work was supported as part of the Quantum-Materials for Energy Efficient Neuromorphic-Computing (Q-MEEN-C), an Energy Frontier Research Center funded by the U.S. Department of Energy, Office of Science, Basic Energy Sciences under Award No. DE-SC0019273. This work used Expanse at San Diego Supercomputer Center (SDSC) through allocation ASC200042 from the Advanced Cyberinfrastructure Coordination Ecosystem: Services & Support (ACCESS) program, which is supported by National Science Foundation Grants No. 1548562 and No. 1445506.

DATA AVAILABILITY

The data that support the findings of this article are not publicly available because they contain commercially sensitive information. The data are available from the authors upon reasonable request.

[1] M. C. Wang and G. E. Uhlenbeck, On the theory of the Brownian motion II, Rev. Mod. Phys. **17**, 323 (1945).

[2] M. Pfützner, M. Karny, L. Grigorenko, and K. Riisager, Radioactive decays at limits of nuclear stability, Rev. Mod. Phys. **84**, 567 (2012).

[3] K. R. Sreenivasan, Fluid turbulence, Rev. Mod. Phys. **71**, S383 (1999).

[4] R. McMichael, D. Twisselmann, and A. Kunz, Localized ferromagnetic resonance in inhomogeneous thin films, Phys. Rev. Lett. **90**, 227601 (2003).

[5] H. Yamamoto, S. Sekikawa, H. Taniguchi, M. Matsukawa, K. Shigematsu, T. Honda, K. Yamauchi, K. Ikeda, T. Otomo, T. Sakakura, M. Azuma, S. Nimori, Y. Noda, and H. Kimura, Reversible thermally controlled spontaneous magnetization switching in perovskite-type manganite, Appl. Phys. Lett. **117**, 112404 (2020).

[6] A. V. Khvalkovskiy, D. Apalkov, S. Watts, R. Chepulskii, R. S. Beach, A. Ong, X. Tang, A. Driskill-Smith, W. H. Butler, P. B. Visscher, D. Lottis, E. Chen, V. Nikitin, and M. Krounbi, Basic principles of STT-MRAM cell

operation in memory arrays, J. Phys. D: Appl. Phys. **46**, 074001 (2013).

[7] W. H. Butler, T. Mewes, C. K. Mewes, P. Visscher, W. H. Rippard, S. E. Russek, and R. Heindl, Switching distributions for perpendicular spin-torque devices within the macrospin approximation, IEEE Trans. Magn. **48**, 4684 (2012).

[8] U. Roy, T. Pramanik, L. F. Register, and S. K. Banerjee, Write error rate of spin-transfer-torque random access memory including micromagnetic effects using rare event enhancement, IEEE Trans. Magn. **52**, 3402106 (2016).

[9] U. Roy, T. Pramanik, S. Roy, A. Chatterjee, L. F. Register, and S. K. Banerjee, Machine learning for statistical modeling: The case of perpendicular spin-transfer-torque random access memory, ACM Trans. Des. Autom. Electron. Syst. **26**, 1 (2021).

[10] H. Risken, Fokker-Planck equation, *The Fokker-Planck Equation: Methods of Solution and Applications* (Springer, New York, 1996).

[11] G. Grimmett and D. Stirzaker, *Probability and Random Processes* (Oxford University Press, Oxford, 2020).

[12] Y. Xie, B. Behin-Aein, and A. W. Ghosh, Fokker—Planck study of parameter dependence on write error slope in spin-torque switching, IEEE Trans. Electron Devices **64**, 319 (2017).

[13] F. T. Arecchi, Measurement of the statistical distribution of Gaussian and laser sources, Phys. Rev. Lett. **15**, 912 (1965).

[14] M. Acharyya and B. K. Chakrabarti, Response of Ising systems to oscillating and pulsed fields: Hysteresis, ac, and pulse susceptibility, Phys. Rev. B **52**, 6550 (1995).

[15] T. Yoshida and K. Enpuku, Simulation and quantitative clarification of ac susceptibility of magnetic fluid in nonlinear Brownian relaxation region, Jpn. J. Appl. Phys. **48**, 127002 (2009).

[16] M. D'Alessandro, A. Tenenbaum, and A. Amadei, Dynamical and statistical mechanical characterization of temperature coupling algorithms, J. Phys. Chem. B **106**, 5050 (2002).

[17] M. H. Gorji, M. Torrilhon, and P. Jenny, Fokker–Planck model for computational studies of monatomic rarefied gas flows, J. Fluid Mech. **680**, 574 (2011).

[18] W. F. Brown, Jr., Thermal fluctuations of a single-domain particle, Phys. Rev. **130**, 1677 (1963).

[19] Z. Lin, I. Volvach, X. Wang, and V. Lomakin, Eigenvalue-based micromagnetic analysis of switching in spin-torque-driven structures, Phys. Rev. Appl. **17**, 034016 (2022).

[20] W. F. Brown, *Micromagnetics* (Interscience Publishers, New York, 1963).

[21] M. D'Aquino, C. Serpico, G. Miano, and C. Forestiere, A novel formulation for the numerical computation of magnetization modes in complex micromagnetic systems, J. Comput. Phys. **228**, 6130 (2009).

[22] J. C. Slonczewski, Current-driven excitation of magnetic multilayers, J. Magn. Magn. Mater. **159**, L1 (1996).

[23] L. Berger, Emission of spin waves by a magnetic multilayer traversed by a current, Phys. Rev. B **54**, 9353 (1996).

[24] J. Xiao, A. Zangwill, and M. D. Stiles, Macrospin models of spin transfer dynamics, Phys. Rev. B **72**, 014446 (2005).

[25] X. Oriols, F. Martín, and J. Suné, Approach to study the noise properties in nanoscale electronic devices, Appl. Phys. Lett. **79**, 1703 (2001).

[26] M. G. Cottam, *Linear and Nonlinear Spin Waves in Magnetic Films and Superlattices* (World Scientific, 1994).

[27] Z. Lin, I. Volvach, and V. Lomakin, Switching current reduction in magnetoresistive random access memories, J. Magn. Magn. Mater. **568**, 170361 (2023).

[28] R. Chang, S. Li, M. V. Lubarda, B. Livshitz, and V. Lomakin, FastMag: Fast micromagnetic simulator for complex magnetic structures (invited), J. Appl. Phys. **109**, 07D358 (2011).

[29] R. B. Lehoucq, D. C. Sorensen, and C. Yang, *ARPACK Users' Guide: Solution of Large-Scale Eigenvalue Problems with Implicitly Restarted Arnoldi Methods* (SIAM, Philadelphia, 1998).

[30] M. Alnæs, J. Blechta, J. Hake, A. Johansson, B. Kehlet, A. Logg, C. Richardson, J. Ring, M. E. Rognes, and G. N. Wells, The FEniCS project version 1.5, Arch. Numer. Softw. **3**, 9 (2015).

[31] A. Logg, K.-A. Mardal, and G. Wells, *Automated Solution of Differential Equations by the Finite Element Method: The FEniCS Book* (Springer Science & Business Media, New York, 2012), Vol. 84.

[32] S. Perna, F. Bruckner, C. Serpico, D. Suess, and M. d'Aquino, Computational micromagnetics based on normal modes: Bridging the gap between macrospin and full spatial discretization, J. Magn. Magn. Mater. **546**, 168683 (2022).